



# Mechanochromic Photonic-Crystal Fibers Based on Continuous Sheets of Aligned Carbon Nanotubes\*\*

Xuemei Sun,\* Jing Zhang, Xin Lu, Xin Fang, and Huisheng Peng\*

**Abstract:** A new family of mechanochromic photonic-crystal fibers exhibits tunable structural colors under stretching. This novel mechanochromic fiber is prepared by depositing polymer microspheres onto a continuous aligned-carbon-nanotube sheet that has been wound on an elastic poly(dimethylsiloxane) fiber, followed by further embedding in poly(dimethylsiloxane). The color of the fiber can be tuned by varying the size and the center-to-center distance of the polymer spheres. It further experiences reversible and rapid multicolor changes during the stretch and release processes, for example, between red, green, and blue. Both the high sensitivity and stability were maintained after 1000 deformation cycles. These elastic photonic-crystal fibers were woven into patterns and smart fabrics for various display and sensing applications.

In nature, creatures such as the chameleon and cuttlefish are renowned for their capability to rapidly change the color of their skin in response to the surrounding environment for camouflage to escape or forage, communication, mood indication, and thermoregulation.<sup>[1,2]</sup> The chromatic transitions typically arise from the translocation of pigments or a rearrangement of reflective units within a large number of chromatophores.<sup>[1]</sup> The translation of natural structures and functionalities to artificial chromic materials and devices has attracted increasing attention owing to a broad spectrum of promising applications, for example, as smart displays or in sensing and actuation. Chromatic transitions in response to light, temperature, chemical species, mechanical deformation, electricity, and magnetic fields have been extensively investigated.<sup>[3–8]</sup> However, the conventional film shape of chromatic materials and devices can hardly live up to the requirements for many applications, such as portable and wearable electronics. To this end, the use of fibers may represent a promising strategy as fibers can be woven into

lightweight fabrics with another unique advantage, namely good breathability.

Several chromic fibers have been realized based on electrochromic materials.<sup>[9–11]</sup> For instance, carbon nanotube/polydiacetylene composite fibers show a color change from blue to red that is due to a change in the conformation of polydiacetylene when an electric current is applied.<sup>[12]</sup> However, the color change could only be reversed for tens of cycles and only a limited number of colors could be displayed (mainly blue and red). Some efforts were also directed towards incorporating different conjugated polymers into the electrochromic layers.<sup>[13]</sup> However, to summarize, the above-mentioned thin electrochromic fibers are not stretchable and easily break during use. Furthermore, electrochromism usually needs a certain voltage, which causes various safety problems, particularly considering that these fibers are in contact with our body in many applications. Therefore, our attention has shifted to mechanochromic materials, which can change color under deformations such as bending and stretching. Mechanochromic devices exhibit several advantages over their competitors: They are safe and also convenient for practical applications as such deformations often occur to wearable electric clothes during motion. Although photonic-crystal-based mechanochromic films have been widely explored,<sup>[14–18]</sup> mechanochromic fibers have hardly been realized. Recently, some attempts were made to produce one-dimensional mechanochromic materials by rolling up a film composed of two dielectric polymers or by extruding core-shell polymer particles.<sup>[19,20]</sup> However, it is difficult to produce a continuous fiber by scrolling a polymer film, and the requirement for hard-soft core-shell polymer nanoparticles during extrusion limits the generalization in preparing desired fiber materials and leads to low color qualities.

Herein, a general and efficient strategy for the preparation of continuous mechanochromic fibers with superior properties is described. The photonic-crystal fiber was made by electrophoretically depositing polymer microspheres, such as polystyrene (PS), onto a continuous sheet of aligned carbon nanotubes (CNTs) that had been wound on an elastic poly(dimethylsiloxane) (PDMS) fiber, followed by further embedding in PDMS. The color of the photonic-crystal fibers, which arise from the assembly of polymer spheres, can be tuned by the size of and the distance between the PS microspheres. In particular, the mechanochromic fiber, with a unique core-sheath structure and an elastic matrix, experiences rapid chromatic transitions during stretch and release processes with a high sensitivity and full reversibility, for example, between the colors red, green, and blue. Both the high sensitivity and stability were maintained even after over

[\*] Dr. X. Sun, J. Zhang, X. Lu, X. Fang, Prof. H. Peng  
State Key Laboratory of Molecular Engineering of Polymers  
Department of Macromolecular Science, and Laboratory of  
Advanced Materials, Fudan University  
Shanghai 200438 (China)  
E-mail: sunxm@fudan.edu.cn  
penghs@fudan.edu.cn

[\*\*] This work was supported by MOST (2011CB932503), NSFC (21225417, 51403038), STCSM (12nm0503200), the China Postdoctoral Science Foundation (2047M560290), the Fok Ying Tong Education Foundation, the Program for Special Appointments of Professors at Shanghai Institutions of Higher Learning, and the Program for Outstanding Young Scholars of the Organization Department of the CPC Central Committee.

Supporting information for this article is available on the WWW under <http://dx.doi.org/10.1002/anie.201412475>.

1000 deformation cycles. The mechanochromic fibers were woven into various patterns and fabrics for potential applications in displays and sensing.

The preparation of mechanochromic fiber is illustrated in the Supporting Information, Scheme S1. First, the elastic fiber was prepared by curing the PDMS precursor in a tube-like mold with a typical diameter of 1.5 mm. Then, the aligned CNT sheets derived from spinnable CNT arrays were wrapped onto an elastic PDMS fiber through a rotation-translation strategy.<sup>[21]</sup> The thickness of the CNT sheath depends on the width and helical angle of the CNT sheets. In the present study, the CNT sheaths had a thickness of approximately 330 nm, and the CNTs were highly aligned on the elastic fiber (Figure S1). The black, conductive CNT sheath endowed the elastic fiber with a high conductivity so that it can be used as the substrate and as an electrode. Afterwards, PS microspheres, with a typical diameter of 200 nm, were deposited onto the elastic fiber by a fast electrophoretic deposition (EPD) process.<sup>[22]</sup> Given that the PS microspheres are negatively charged, the conductive elastic fiber was used as the anode with a stainless steel plate as the counter electrode. When an electric field was applied, the PS microspheres migrated towards the conductive elastic fiber and rapidly assembled into a colloidal crystal structure.<sup>[22]</sup> Later, PS microspheres were embedded in the PDMS precursors and cured to form the elastic photonic-crystal fiber. Finally, the mechanochromic photonic-crystal fiber was obtained after swelling and thermally grafting the vinyl-terminated silicon oil to the PDMS backbone. As the syntheses of the PS microspheres, the aligned CNTs, and the PDMS substrate are technically mature processes, the whole process is facile and fast and may be easily implemented in an industrial setting.

In this fabrication process, the employed EPD method represents one of the most effective processes for colloidal assembly to form photonic crystals, but it requires an electrically conductive substrate.<sup>[22]</sup> No fiber-shaped mechanochromic photonic crystals have been produced thus far owing to a lack of elastic and conductive fiber substrates. The surface morphology of the substrate also plays an important role in the EPD process.<sup>[23]</sup> In our process, an elastic and conductive fiber substrate was obtained by winding aligned CNT sheets onto the PDMS fiber, and the aligned structure can be well maintained with a stable resistance under stretching and releasing (Figure S1). The aligned structure of the CNTs is crucial as it is responsible for both the high conductivity and mechanical stability. When randomly dispersed CNTs were used, the resulting fibers showed uneven surfaces with large aggregates (Figure S2). Upon stretching, the random CNTs were ruptured with a distinct increase in resistance, and the original resistance value could not be recovered after strain release (Figure S3). In another control experiment, conductive graphene was coated onto the elastic fiber. Unfortunately, the resulting fiber became stiff; the graphene sheets cracked and peeled off from the PDMS substrate under stretching (Figure S4).

The morphology of the 200 nm PS colloidal crystals on the conductive elastic fiber is shown in Figure 1a. The PS microspheres were uniformly deposited with a close-packed

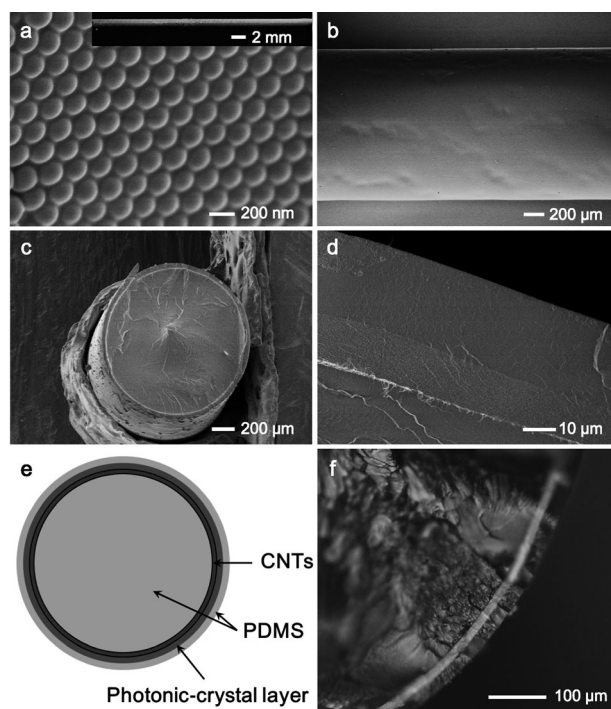


**Figure 1.** Scanning electron microscopy (SEM) images of mechanochromic fibers. a) The assembled 200 nm PS microspheres. Inset: Photograph of the fiber after deposition of the PS microspheres. b) Side view of the elastic mechanochromic fiber. c, d) Cross-sectional view of the fiber in (b) at low (c) and high (d) magnification. e) Schematic illustration of the cross-sectional structure of the mechanochromic fiber. f) Cross-sectional optical micrograph of the mechanochromic fiber. The light-colored section in the image indicates the 200 nm PS microspheres that were deposited on the CNT sheets and embedded in PDMS.

structure on the surface and displayed a blue color (Figure 1a, inset). The aligned CNTs beneath the photonic-crystal layer also affected the color of the fiber. As shown in Figure S5, when the thickness of the aligned CNTs was increased from approximately 40 and 100 to about 300 nm, the color of the fiber under otherwise identical conditions became more and more vivid owing to absorption by the CNTs, which act like a black background.<sup>[24]</sup> Importantly, the reflection spectra were similar because the reflection is mainly due to the PS microspheres. After infiltration with PDMS, the fiber had a uniform and smooth surface where the PS microspheres were embedded completely (Figure 1b). The core–sheath structure of the resulting fiber can be clearly seen in the cross-sectional images obtained with different microscopes. The PS microspheres and the CNT sheets, which formed a layer with a thickness of approximately 15  $\mu\text{m}$ , were sandwiched between the inner PDMS fiber and an outer PDMS layer (Figure 1c–f; see also Figure S6). The high PDMS volume fraction (ca. 98%) leads to a highly sensitive elastic fiber, which will be discussed later. In addition, only a very thin layer of the photonic crystal was required to obtain the desired color.<sup>[22]</sup>

The diameter of the PS microspheres exerts an influence on the initial colors and reflection peaks of the fiber. Bragg's

equation was thus used to elucidate the displayed color. When the PS microspheres are stacked into a face-centered cubic (fcc) colloidal crystal, the wavelength of the reflection peaks can be approximately calculated by  $\lambda = 2dn_{\text{eff}} = (8/3)^{1/2}D(0.74n_p^2 + 0.26n_m^2 - \sin^2\theta)^{1/2}$ , where  $d$ ,  $n_{\text{eff}}$ ,  $D$ ,  $n_p$ ,  $n_m$ , and  $\theta$  correspond to the (111) plane spacing, the effective refractive index, the diameter of the polymer spheres, the refractive index of the polymer spheres, the refractive index of the matrix, and the angle between the incident beam and the [111] direction of stacking, respectively.<sup>[25]</sup> Accordingly, when the incident light entered the fiber along its radial direction, colloidal crystals made from PS microspheres ( $n_p = 1.59$ ,  $n_m = 1$ ) with diameters of 200, 220, 240, 260, and 280 nm should exhibit reflection peaks at wavelengths of 476, 524, 572, 619, and 667 nm, respectively. In fact, the measured spectra displayed reflection peaks at 448, 509, 533, 573, and 624 nm, respectively (Figure S7). The blue shift with respect to the theoretical prediction was attributed to the reduction of the diameter of the PS microspheres during the drying process, which was deduced to amount to approximately 4.9% from the experimental results.<sup>[26]</sup> The defects and the curved surface led to a slight broadening of the peaks in the reflection spectra compare to those of the ideal structure. After the fibers had been filled with PDMS elastomer and further grafted with silicon oil, the reflection peaks shifted to longer wavelengths, that is, from 448 to 493 and 531 nm for the 200 nm PS microspheres, and from 533 to 575 and 646 nm for the 240 nm PS microspheres (Figure S8). These reflection peaks are in line with the color transitions from blue to green and from green to red, which are caused by changes to the matrix and the increase in the center-to-center distance between the PS microspheres. As a result, the colors of the elastic photonic-crystal fibers depend on the size of deposited microspheres. A green and a red fiber, which were derived from 200 and 240 nm PS microspheres, respectively, are shown in Figure 2c and e.

Benefiting from its rubbery matrix, the photonic-crystal fiber has a decent elasticity, which enables the elongation of the fiber to produce color changes. As illustrated in Figure 2a and b, when stretched, the photonic-crystal fiber was axially elongated and shrunk radially; therefore, the lattice constants of the assembled PS microspheres increase in the axial direction and decrease in the radial direction. Given that the fiber color appeared selectively as a result of light diffraction in the radial direction, which complies with Bragg's rule, the reflection peak was shifted to a shorter wavelength under stretching. The color changes of the elastic photonic-crystal fibers from green to blue and from red to green under a mechanical strain of 30% are shown in Figure 2c–f. After release, the elastic photonic-crystal fiber regained its original color, which indicates that the structural color transition is reversible.

The reversibility of the stretch/release deformations was examined for both bare PDMS and elastic photonic-crystal fibers (Figure S9). The stress of the photonic fiber was found to be larger than that of a bare PDMS fiber under the same strain, possibly owing to the presence of the stiff CNTs and PS microspheres. When stretched to a strain of 40%, both fiber materials could fully recover their original shapes after strain

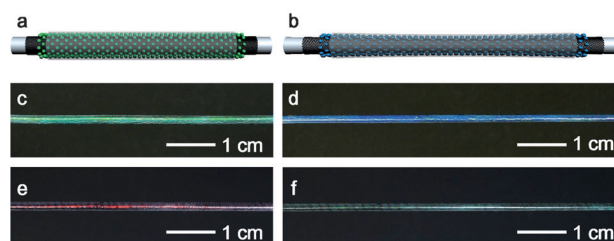


**Figure 2.** Mechanochromic fibers. a, b) Schematic illustration of the structure changes of the fiber under stretching. c, d) Photographs of the mechanochromic fiber made from 200 nm PS microspheres before (c) and after (d) stretching. e, f) Photographs of the mechanochromic fiber made from 240 nm PS microspheres before (e) and after (f) stretching.

release, and the above process could be repeated thousands of times, indicating the high elasticity and stability of the materials. After stretching to 100% or more and subsequent release, the bare PDMS fiber immediately fully recovered its original shape; a slight residual strain of approximately 5% was detected for the photonic-crystal fiber, which, however, still quickly recovered its original shape.

The mechanochromic behavior of the elastic photonic-crystal fiber was then characterized by reflection spectroscopy. The evolution of the reflection spectra of the fiber during the stretching process is displayed in Figure 3a and c. Irrespective of whether the fibers were made from 200 nm or 240 nm PS microspheres, the reflection peaks were shifted to shorter wavelengths, and the reflection intensities gradually decreased. The dependence of the reflection peak on the strain of the fiber made from 200 nm PS microspheres is illustrated in Figure 3b, and the peak was shifted from 531 to 449 nm when the fiber was elongated by 30%. There was no distinctive change in the reflection peak upon further stretching, implying that the PS microspheres were in contact with each other in the radial direction and that no interval spaces were available for a change in structure. Similar results were obtained for the fiber made from 240 nm PS microspheres. Its reflection peak shifted from 646 to 545 nm with an increase in strain from 0 to 35%, but no changes were observed for a further increase in strain (Figure 3c). The mechanochromic sensitivity, which is defined as  $\Delta\lambda/\Delta\epsilon$  (the change in the reflection peak relative to the percentage elongation), was measured to be approximately 2.8 nm/% on average for the photonic-crystal fiber and thus found to be much higher than that of the photonic-crystal films.<sup>[14,18]</sup> The mechanochromic behavior of the elastic photonic-crystal fiber had a remarkable reversibility. As demonstrated in Figure 3d, after the mechanical strain had been removed, the reflection peak of the photonic-crystal fiber returned to its original position. The transition could be repeated for over 1000 cycles with strains between 0 and 15%, indicating that the structure of the elastic photonic-crystal fiber is highly stable.

Upon stretching with a strain  $\epsilon$ , the lattice constants of the assembled PS microspheres decrease to  $1 - \nu\epsilon$  in the radial direction where  $\nu$  is the Poisson ratio of the fiber.<sup>[27]</sup> The position of the reflection peak can then be linearly expressed



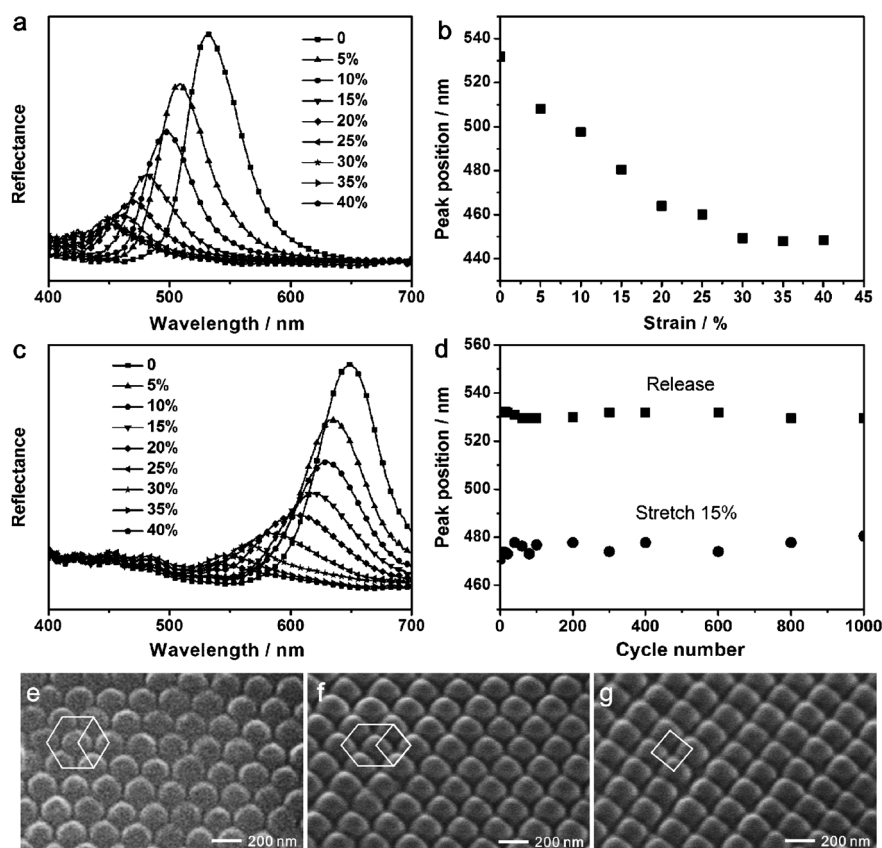


**Figure 3.** Mechanochromic performance of the elastic photonic-crystal fiber. a) Reflection spectra of the fiber made from 200 nm PS microspheres under different strains. b) Variation of the peak position with strain in (a). c) Reflection spectra of the fiber made from 240 nm PS microspheres under different strains. d) Evolution of the peak position over 1000 cycles of stretching (15% strain) and releasing. The elastic photonic-crystal fiber was prepared with 200 nm PS microspheres. e–g) SEM images of a colloidal crystal layer on the surface before (e) and after stretching to 30% (f) and 50% (g). The fiber was stretched along the horizontal direction.

as  $\lambda_e = 2d_{111}n_{\text{eff}} = \lambda_0(1 - \nu\epsilon)$ , where  $\lambda_0$  and  $\lambda_e$  are the reflection peaks of the fiber prior to and under stretching. This equation explains the blue shift of the color under stretching. By fitting the experimental data to this equation, a  $\nu$  value of approximately 0.455 was calculated for a strain of less than 30%, which is much higher than the value reported for a mechanochromic film and close to that of the bare PDMS elastomer (0.5), suggesting that the photonic-crystal fiber was homogeneously stretched like an elastic material.<sup>[18,27]</sup> This conclusion was corroborated by the increase in the axial distance between the PS spheres when the material was stretched by 30% (Figure 3e,f). At the same time, the lattice distance in the radial direction of the fiber must decrease until the PS microspheres are in contact with each other, which explains the blue shift of the reflection peaks. At higher strains, for example, at 50% strain, the arrangement of the microspheres changed from hexagons to squares (Figure 3g), similar to the previously reported film.<sup>[27]</sup> The decay of the reflection intensity is primarily attributed to the decrease in the optical dielectric contrast between the PS spheres and PDMS under stretching and possibly also to the order loss in the radial direction of the PS colloidal crystal.<sup>[28,29]</sup> After release, the

elastic PDMS substrate recovered its original arrangement benefitting from the core–sheath structure of the fiber with a thin photonic-crystal sheath (thickness ca. 15  $\mu\text{m}$ ) and a thick PDMS fiber core (diameter 1.5 mm). The relation between  $\lambda$  and  $\epsilon$  can then be expressed as  $\lambda_e = \lambda_0(1 - 0.455\epsilon)$  for strains of  $\leq 30\%$ ; the wavelength of the reflection peak can thus be tuned by varying the strain of the fiber.

Owing to its one-dimensional configuration and mechanochromic properties, the elastic photonic-crystal fiber may find applications in displays and sensing devices. For example, the fibers can be woven into chromatic fabrics for fashionable and individual wearable items, avoiding the use of organic dyes or pigments. In Figure 4a–c, several colorful patterns that were prepared with different elastic photonic-crystal fibers are shown. Owing to their intrinsic structural color, the patterns are fade-resistant and durable. Moreover, the mechanochromic performance makes the fiber sensitive and responsive to mechanical strain, which can be used to map the stress distribution or to monitor the movement of a body, for example. A fabric cross-woven from green and red elastic photonic-crystal fibers is shown in Figure 4d–g. Four color combinations can be realized by application of various strain combinations. For instance, when stretched in the vertical direction, the fabric became

red and blue as the green fibers turned blue, whereas it only displayed a green color on stretching in the horizontal direction because the red fibers turned green. When bilaterally stretched at the same time, the fabric displayed the colors green and blue. As a pH test paper can indicate the acidity and alkalinity in color, the mechanochromic photonic-crystal fiber can visualize the applied strain as a load sensor. As shown in Figure S10, fibers loaded with different weights exhibited different colors. Once a correlation between the weight and the position of the reflection peak of the fiber has been established, it will be a viable approach to visualize the load.

The observed color varied in the radial direction, with the middle section appearing to be brighter than the side as they were not in the same plane owing to the curved fiber surface. This iridescence phenomenon has been intensively studied for highly ordered photonic crystals. To suppress the iridescence effects, two PS microspheres with different diameters were simultaneously deposited onto an aligned CNT sheet to form a disordered structure (Figure S11).<sup>[30,31]</sup> More efforts are underway to achieve bright and saturated colors in mimicking nature.

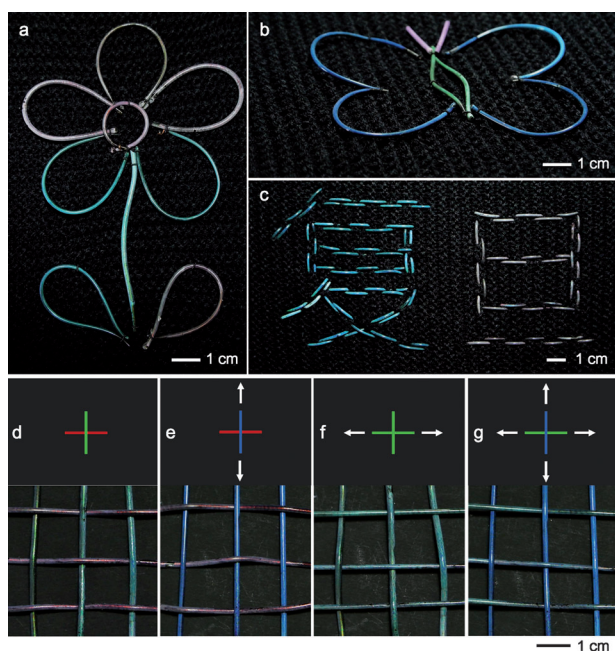


**Figure 4.** Chromatic patterns and fabric made from elastic photonic-crystal fibers. a–c) Colorful patterns woven from different photonic-crystal fibers. d–g) Schematic illustration and photographs of the mechanochromic fabrics under different manipulations in their initial state (d), under vertical stretching (e), under horizontal stretching (f), and under bilateral stretching (g).

In conclusion, a new family of multicolored mechanochromic photonic-crystal fibers was synthesized by a fast and facile process. These fibers exhibit brilliant color changes and obvious reflection peak shifts in the visible-light range under mechanical strains from 0 to 30% and maintained very high sensitivity, reversibility, and stability for thousands of cycles owing to the unique core–sheath structure. These elastic photonic-crystal fibers can be woven into smart fabrics with promising applications as fashionable displays and for strain mapping and sensing. A general and effective route for the industrial production of novel photonic-crystal fibers has also been presented.

Received: January 2, 2015

Published online: February 27, 2015

**Keywords:** carbon nanotubes · fibers · materials science · mechanochromic properties · photonic crystals

- [1] A. V. Singh, A. Rahman, N. V. G. Sudhir Kumar, A. S. Aditi, M. Galluzzi, S. Bovio, S. Barozzi, E. Montani, D. Parazzoli, *Mater. Des.* **2012**, 36, 829.
- [2] D. Stuart-Fox, M. J. Whiting, A. Moussalli, *Biol. J. Linn. Soc.* **2006**, 88, 437.

- [3] J. Ge, Y. Yin, *Angew. Chem. Int. Ed.* **2011**, 50, 1492; *Angew. Chem.* **2011**, 123, 1530.
- [4] J. Cui, W. Zhu, N. Gao, J. Li, H. Yang, Y. Jiang, P. Seidel, B. J. Ravoo, G. Li, *Angew. Chem. Int. Ed.* **2014**, 53, 3844; *Angew. Chem.* **2014**, 126, 3923.
- [5] K. Hwang, D. Kwak, C. Kang, D. Kim, Y. Ahn, Y. Kang, *Angew. Chem. Int. Ed.* **2011**, 50, 6311; *Angew. Chem.* **2011**, 123, 6435.
- [6] C. G. Schäfer, M. Gallei, J. T. Zahn, J. Engelhardt, G. P. Hellmann, M. Rehahn, *Chem. Mater.* **2013**, 25, 2309.
- [7] X. Sun, T. Chen, S. Huang, L. Li, H. Peng, *Chem. Soc. Rev.* **2010**, 39, 4244.
- [8] Y. Zhao, Z. Xie, H. Gu, C. Zhu, Z. Gu, *Chem. Soc. Rev.* **2012**, 41, 3297.
- [9] X. Sun, Z. Zhang, X. Lu, G. Guan, H. Li, H. Peng, *Angew. Chem. Int. Ed.* **2013**, 52, 7776; *Angew. Chem.* **2013**, 125, 7930.
- [10] P. M. Beaujuge, J. R. Reynolds, *Chem. Rev.* **2010**, 110, 268.
- [11] W. M. Kline, R. G. Lorenzini, G. A. Sotzing, *Color. Technol.* **2014**, 130, 73.
- [12] H. Peng, X. Sun, F. Cai, X. Chen, Y. Zhu, G. Liao, D. Chen, Q. Li, Y. Lu, Y. Zhu, Q. Jia, *Nat. Nanotechnol.* **2009**, 4, 738.
- [13] K. Li, Q. Zhang, H. Wang, Y. Li, *ACS Appl. Mater. Interfaces* **2014**, 6, 13043.
- [14] E. P. Chan, J. J. Walsh, A. M. Urbas, E. L. Thomas, *Adv. Mater.* **2013**, 25, 3934.
- [15] D. Yang, S. Ye, J. Ge, *Adv. Funct. Mater.* **2014**, 24, 3197.
- [16] H. Feng, J. Lu, J. Li, F. Tsow, E. Forzani, N. Tao, *Adv. Mater.* **2013**, 25, 1729.
- [17] F. Castles, S. M. Morris, J. M. C. Hung, M. M. Qasim, A. D. Wright, S. Nosheen, S. S. Choi, B. I. Outram, S. J. Elston, C. Burgess, L. Hill, T. D. Wilkinson, H. J. Coles, *Nat. Mater.* **2014**, 13, 817.
- [18] H. Fudouzi, T. Sawada, *Langmuir* **2006**, 22, 1365.
- [19] M. Kolle, A. Lethbridge, M. Kreysing, J. J. Baumberg, J. Aizenberg, P. Vukusic, *Adv. Mater.* **2013**, 25, 2239.
- [20] C. E. Finlayson, C. Goddard, E. Papachristodoulou, D. R. Snoswell, A. Kontogeorgos, P. Spahn, G. P. Hellmann, O. Hess, J. J. Baumberg, *Opt. Express* **2011**, 19, 3144.
- [21] Z. Yang, J. Deng, X. Sun, H. Li, H. Peng, *Adv. Mater.* **2014**, 26, 2643.
- [22] N. Zhou, A. Zhang, L. Shi, K.-Q. Zhang, *ACS Macro Lett.* **2013**, 2, 116.
- [23] Z. Liu, Q. Zhang, H. Wang, Y. Li, *Nanoscale* **2013**, 5, 6917.
- [24] Z. Shen, L. Shi, B. You, L. Wu, D. Zhao, *J. Mater. Chem.* **2012**, 22, 8069.
- [25] Z. Liu, Q. Zhang, H. Wang, Y. Li, *Chem. Commun.* **2011**, 47, 12801.
- [26] A. L. Rogach, N. A. Kotov, D. S. Koktysh, J. W. Ostrander, G. A. Ragoisha, *Chem. Mater.* **2000**, 12, 2721.
- [27] B. Viel, T. Ruhl, G. P. Hellmann, *Chem. Mater.* **2007**, 19, 5673.
- [28] K. Matsubara, M. Watanabe, Y. Takeoka, *Angew. Chem. Int. Ed.* **2007**, 46, 1688; *Angew. Chem.* **2007**, 119, 1718.
- [29] J. F. Bertone, P. Jiang, K. S. Hwang, D. M. Mittleman, V. L. Colvin, *Phys. Rev. Lett.* **1999**, 83, 300.
- [30] J.-G. Park, S.-H. Kim, S. Magkiriadou, T. M. Choi, Y.-S. Kim, V. N. Manoharan, *Angew. Chem. Int. Ed.* **2014**, 53, 2899; *Angew. Chem.* **2014**, 126, 2943.
- [31] L. Shi, Y. Zhang, B. Dong, T. Zhan, X. Liu, J. Zi, *Adv. Mater.* **2013**, 25, 5314.